ENGINEERING TRANSACTIONS • *Engng. Trans.* • **49**, 2–3, 213–240, 2001
Polish Academy of Sciences • Institute of Fundamental Technological Research
10.24423/engtrans.555.2001

MODELLING ELASTIC BEHAVIOUR OF SOFT TISSUES PART I. ISOTROPY

S. JEMIOŁO [1] and J. J. TELEGA [2]

[1] **INSTITUTE OF STRUCTURAL MECHANICS**
WARSAW UNIVERSITY OF TECHNOLOGY
al. Armii Ludowej 16, 00–637 Warsaw, Poland
e-mail: s.jemiolo@il.pw.edu.pl

[2] **INSTITUTE OF FUNDAMENTAL TECHNOLOGICAL RESEARCH**
POLISH ACADEMY OF SCIENCES
Świętokrzyska 21, Warsaw, Poland
e-mail: jtelega@ippt.gov.pl

Soft tissues mostly exhibit strongly nonlinear behaviour while undergoing large strains. New macroscopic models for both isotropic and transversely isotropic soft tissues have been proposed. The models developed are suitable for finite element formulation. It the first part of the paper isotropic models have been proposed. Implementation in the FEM programme ABAQUS has been discussed. Muscle contraction models have also been concisely reviewed.

1. INTRODUCTION

Common feature of soft tissues is their nonlinear behaviour in the range of moderate and large deformations, cf. [6, 15 – 17, 23, 25 – 29, 38 – 40, 42, 44, 45, 48, 50 – 53, 61, 69, 73, 74, 77] and Part II of our paper. Anyway, at the macroscopic level, the behaviour of such tissues involves hyperelasticity. Only this aspect will be examined in the present paper. We shall not examine the cycle loading-unloading and the influence of fluids, cf. [63 – 65]. In our opinion, prior to study the macroscopic behaviour of soft tissues treated as poroelastic material one has to elaborate appropriate hyperelastic models. Another challenging problem

which arises is due to the presence of residual stresses and strains, cf. [2, 12, 16] and the second part our paper. This fact implies that, rigorously speaking, the natural configuration for soft tissues is not easily accessible. Nevertheless, in our subsequent considerations the natural configuration is defined in a standard manner.

The aim of the present contribution is twofold. First, we provide a concise overview of muscle contraction models. Second, we propose new isotropic hyperelastic models suitable for modelling the macroscopic behaviour of soft tissues. Our models generalises the one elaborated by FUNG [15], see also the relevant references therein. We observe that the computational framework for finite element implementation of isotropic hyperelastic models was developed in ABAQUS [1]. The interface UHYPER with Fortran codes of the stored energy function (5.5), (5.6) with their derivatives, with respect to the strain invariants, is also available [36, 38]. Tests problems were solved to demonstrate the utility and accuracy of the implementation. The material constants were taken from experiments on rabbit aorta [65]. For others models of soft tissues the reader is referred to the papers already cited and to Part II.

We observe that in modelling muscles one may distinguish three main approaches. The first approach, at the lowest (molecular) level of modelling is focussed on muscle contraction, as viewed from the point of biophysics, cf. [15, 31 – 35, 66 – 68]. The second approach to muscle contraction modelling was initiated by HILL [19], cf. also FUNG [15] for historical comments on earlier investigations. The third approach is purely phenomenological, typical for solid mechanics. In this paper we follow the third approach. It seems that with the advent of the so-called formation theory [62], it will be possible to incorporate the basic structural units of skeletal muscles or the sarcomeres into macroscopic models. More precisely, in our opinion the sarcomeres can be treated as microactuators. However, this is a program for the future.

The class of soft tissues comprises not only striated and smooth muscles but also the heart muscle, eye tissue, blood vessels, skin, lungs, ligaments, tendons, cartilage, etc. For details the reader is referred to [5, 13, 17, 30, 40 – 45, 49, 78, 79]. The remarkable book by YAMADA [80] gathers in one volume the data on strength of tissues and mechanical properties of organs up to 1970.

2. MORPHOLOGY OF SKELETAL MUSCLE

There are three kinds of muscles: skeletal, heart, and smooth muscles, cf. [15]. Skeletal and heart muscles are striated muscles. Muscles in which striations cannot be seen are called smooth muscles, cf. [59]. Among them are vascular

smooth muscles and intestinal smooth muscles. Muscles are soft tissues. The class of soft tissues is large; it also comprises tissues so different as skin, ureter, blood vessels, lung parenchyma, kidney, eye tissue, cartilage, etc. Except the cartilage, all these tissues reveal strongly nonlinear behaviour in the range of large deformations. The cartilage is often treated as a linear material, though in the range of large deformations its response is also nonlinear though not so strongly as say skeletal muscles. We recall that a tissue is a collection of cells and extracellular matrices, that perform specialized functions. The extracellular matrix consist of fibers (e.g., the proteins collagen and elastin) and a ground substance (e.g., proteoglycans in cartilage). Animal tissues are classified into four main groups: connective, epithelial, muscle, and nerve, cf. [11] and the references therein. A *connective tissue* is defined as *any* tissue in which the proportion of extracellular matrix occupies a greater volume than the cellular component. Connective tissue include cartilage, tendons, ligaments, the matrix of bone, and the adipose (fatty) tissues as well as skin, blood, and lymph. Blood and lymph are special connective tissues where the extracellular matrix is a fluid component.

Different organs have different smooth muscles: there are sufficient difference among these muscles anatomically, functionally and in their responses to drugs. However, there are also common features. All muscles, skeletal, heart, and the various smooth muscles, contain *actin* and *myosin*, see below. All rely on ATP (adenosine triphosphate) for energy.

In the first part of the paper we shall be concerned with isotropic models of soft tissues. In the present section we shall be deliberately concerned with the morphology of skeletal muscle. It is not possible to discuss the morphology of all important soft tissues in one paper. This section will also reveal important for the second part of the paper. Skeletal muscles are inherently anisotropic. However, in Part II of our paper we shall see that constitutive relations for anisotropic soft tissues usually contain an isotropic part. Also, some soft tissues are sufficiently accurately modelled as isotropic materials, for instance, see [40, 41, 74].

Let us pass now to the presentation of skeletal muscle morphology. The skeletal muscle, similar to other tissues, exhibits a hierarchical structure, cf. Fig. 1. A brief look into an anatomical atlas reveals an enormous diversity in muscle architectures. However, the units of skeletal muscle are the muscle fibres, each of which is a single contractile muscle cell provided with many hundreds of nuclei [9, 15, 68]. These fibers are arranged in bundles or *fasciculi* of various sizes within the muscle. The muscle fibers are also referred to as *myocytes*. Macroscopically, the other main constituents of a skeletal muscle are the passive stiff nonlinear elastic collagen tissues: *aponeuroses* and tendons. Aponeuroses or tendinous sheets are macroscopically organised as membranes to which muscle fibers are attached.

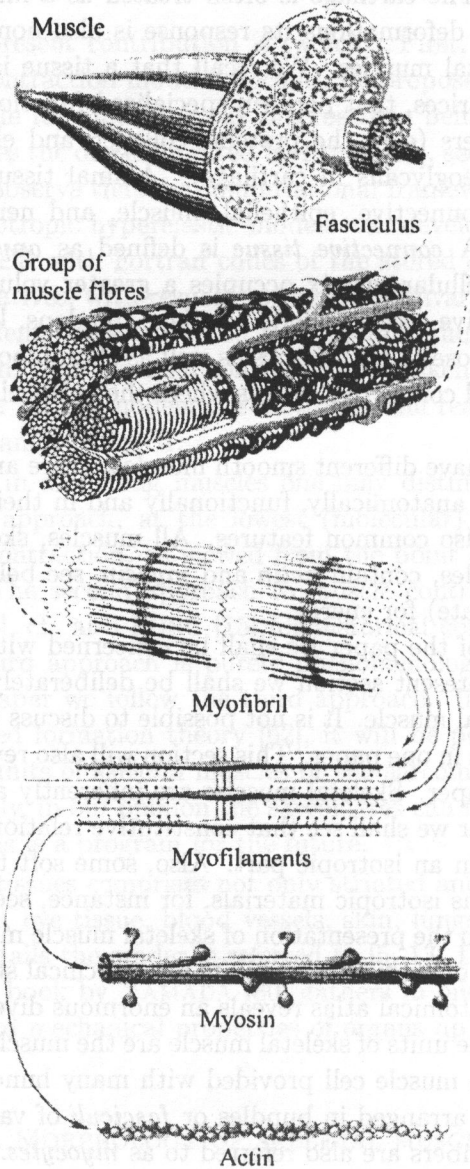

FIG. 1. The organizational hierarchy of skeletal muscle, after [15].

Aponeuroses and muscle fibers connect to bone directly or via tendons, bundled continuations of aponeuroses. Connective tissues run parallel to the active muscle components at each level of detail. The *epimysium* or *fascia*, a strong connective tissue layer, completely surrounds the muscle, whereas *perimysium* separates bundles of fibers and *endomysium* covers and electrically isolates individual fibers. Epi-peri- and endomysium interconnect and continue in aponeuroses and tendons. They are important for serial as well as for lateral force transmission.

Some muscles, like human sartorius muscle, are slender and contain long fibers in series with short tendons. The fibers of this muscle are oriented parallel to the line of pull of the muscle. Muscles like sartorius muscle generate low forces. However, due to the length of their fibers they can exert force over a large length range. Other muscles, like human gastrocnemius muscle, have many short fibers in parallel that make a considerable angle with the line of pull of the muscle. In the gastrocnemius muscle the fibers are attached to the long and compliant Achilles tendon. Muscles like the gastrocnemius muscle are particularly suitable for generating high forces, albeit over a small length range.

A skeletal muscle fiber is elongated, having a diameter of $10 - 60$ μm, and a length usually of several millimeters to several centimeters; but sometimes the length can reach 30 cm in long muscles. The fibers may stretch from one end of the muscle to another, but often extend only in tendinous or other connective tissue intersections.

The flattened nuclei of muscle fibers lie immediately beneath the cell membrane. The cytoplasm is divided into longitudinal threads or *myofibrils*, each about $1 - 2$ μm in diameter, that extend over the entire length of the fiber. These myofibrils are striated when they are stained by dyes and when they are examined optically. Some zones stain lightly with basic dyes such as hematoxylin, rotate the plane of polarization of light weakly, and are called *isotropic* or *I bands*, cf. Fig. 2. Others, alternating with the former, stain deeply with hematoxylin and strongly rotate the plane of polarization of light to indicate a highly ordered substructure. They are called *anisotropic* or *A bands*. The I bands are bisected transversely by a thin line also stainable with basic dyes: this line is called the *Zwischenscheible* or *Z band*. The A bands are also bisected by a paler line called the *H band*. All these bands are illustrated in Fig. 2.

Each myofibril is composed of arrays of *myofilaments*. These are divided transversely by the Z bands into serially repeating regions termed sarcomeres, each about 2.4 μm long, with the exact length dependent on the force acting in the muscle and the state of excitation. Two types of myofilament are distinguishable in each sarcomere, the fine ones about 5 nm in diameter and the thicker ones about 12 nm across. The fine ones are actin molecules about 1.0 μm long, having a helical structure. The thick ones are myosin molecules about 1.6 μm long, also

having a helical structure. The actin filaments are each attached at one end to a Z band and are free at the other to interdigitate with the myosin filament. The spatial arrangements of these fibers are shown in Figs. 1, 2. It is seen that the A

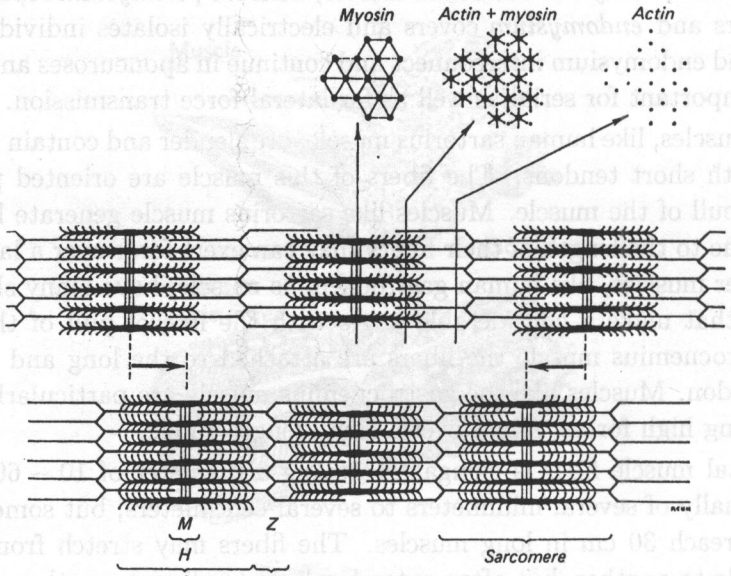

FIG. 2. The structure of myofilament showing the spatial arrangement of the actin and myosin molecules, after [15].

band is the band of myosin filaments, and the I band is the band of the parts of the actin filaments that do not overlap with the myosin. The H bands are the middle region of the A band into which the actin filaments have not penetrated. Another line, the M band, lies transversely across the middle of the H bands, and close examination shows this to consist of fine strands interconnecting the adjacent myosin filaments. The hexagonal pattern of arrangement of these filaments is shown in Fig. 3a, b. Each myosin filament consists of about 180 myosin molecules. Each molecule has a molecular weight of about 500 000 and consists of a long tail piece and a "head", which on close examination is seen to be a double structure, cf. Fig. 3c. On further treatment the molecule can be broken into two moieties: *light meromyosin*, consisting of most of the tail, and *heavy meromyosin* representing the head with part of the tail. The myofilament is formed by the tails of the molecules which lie parallel in bundle, with their free ends directed toward the midpoint of the long axis. The heads project laterally from the filament in pairs, at 180° to each other and at 14.3 nm intervals. Each pair is rotated by 120° with respect to its neighbours to form a spiral pattern along the filament. These heads seem to be able to nod: they lie close to their parent filament in relaxation, but

stick out to actin filaments when excited. They are called *cross-bridges*, cf. [15, 31, 66], and the next section.

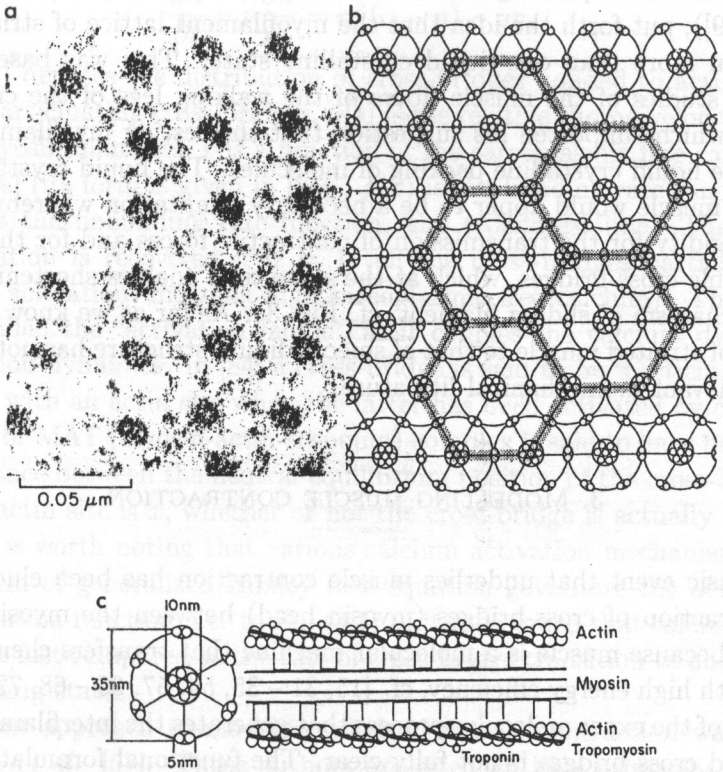

FIG. 3. (a) Cross section of myofibral, as seen from the end. The thick filament myosin, and thin filament, actin, lie beside one another in a hexagonal array (June beetle); (b) Schematic drawing of how the actin and myosin are arranged, as visualized from the electron micrograph (a); (c) Schematic drawing of the longitudinal section, showing actin associated with tropomyosin and myosin. These are three major proteins of muscle myofibrils, after [9].

As we already know, sarcomeres are organized in series into structures called myofibrils. Myofibrils of a typical muscle fiber contain thousands of sacromeres in series. Just to give an impression, fibers of the human quadriceps muscle have over 40000 sarcomers in series, cf. MEIJER [54].

The signal that initiates the event of muscle contraction is the release of calcium ions from the membrane-bound storage sites by the arrival at the muscle of a nerve impulse. The signal is detected and acted on by two additional proteins, *tropomyosin* and *troponin*, which are positioned along the actin filament, cf. BROWN and WOLKEN [9]. It is believed that the calcium ions bind to troponin, which then modifies the positions of the tropomyosin molecule, so that myosin can make contact with the actin molecules.

Another interesting feature of striated muscle was suggested by Nedham in 1950, cf. BROWN and WOLKEN [9]. This author claims that such a muscle is similar to a *smectic liquid crystal structure*. Later, in 1975 April (see BROWN and WOLKEN [9]), put forth the idea that the myofilament lattice of striated muscle can exist in more than one liquid crystalline state. This was based on X-ray diffraction studies of the muscle fibers of the walking legs of the crayfish (*Orconectes*), which supported his suggestion that the resting myofilaments form a smectin-like liquid crystalline packing of molecules. The liquid crystalline lattice of striated muscle would apper to be a necessary adaptation whereby the lattice provides rigidity for the transmission of contractile forces and for the anchoring of the flexible cross-bridges, which at the same time enables shortening to occur by the mechanism of sliding filament, cf. Fig. 3c. As far as we know, the idea of similarity of striated muscle to that of smectic liquid structure has not penetrated into the relevant biomechanical literature.

3. MODELLING MUSCLE CONTRACTION

The basic event that underlies muscle contraction has been elucidated as a cyclic interaction of cross-bridges (myosin head) between the myosin and actin filaments, because muscle is a molecular machine that transfers chemical energy to work with high energy efficiency, cf. [15, 31 – 35, 54, 57, 66 – 68, 72]. However, the nature of the exact molecular process that generates the interfilamentary force by attached cross-bridges is not fully clear. The functional formulation employing state variables as the viscoelasticity model was adopted for the constitutive equation of living tissues in [46]. In such a model the generation and dissipation processes of energy and the zero-stress state were not made clear. A muscle contraction model based on molecular structure was proposed by HUXLEY [31], cf. also [35] and ZAHALAK and MA [83]. Such models owe much to electron microscope observations of the cross-bridge [18, 61], and tension response to sudden length change [14]. However, recent experimental results of the sliding length during one adenosine triphosphate (ATP) hydrolysis do not confirm these models [71, 81].

TORELLI [70] developed a mathematically rigorous model related to muscle contraction and based on Huxley's sliding filament theory. Though being mathematically complicated, the model is strongly simplified. For instance, the myosin filament was assumed to remain rigid. The myofilaments are also rigid in the model developed by ZAHALAK and MOTABARZADEH [84]. In fact, the last model is a refinement of the model previously proposed by ZAHALAK and MA [83] for providing a relation between calcium-activation kinetics and Huxley-type cross-

bridge models. The generalized Huxley equation obtained in [83, 84] with calcium activation has the following form:

$$\frac{\partial n}{\partial t} - \nu \frac{\partial n}{\partial t} = rf(\alpha - n) - gn, \tag{3.1}$$

where $n(x,t)$ denotes the distribution of cross-bridges bonded to actin, α is the fraction of participating cross-bridges, $\nu(t)$ is the relative sliding velocity between actin and myosin filaments, r is a function of the sarcoplasmic free calcium concetration [Ca] (its form is given in [84]), $f(x)$ is the bonding rate function while $g(x)$ denotes the unbonding rate function, and t denotes time. The standard Huxley equation is recovered if $\alpha = 1$ (all the cross-bridges participate) and $r = 1$ (high activation, meaning high sarcoplasmic free calcium). The function $r([\mathrm{Ca}])$ is called the "activation factor", as it couples the calcium dynamics to the contraction dynamics. In [84] a cross-bridge is said to be "participating" if it can interact with an actin site when the latter has been activated by calcium. A cross-bridge or MAT (myosin-actin-troponin) complex is said to have bond length x if the distance between the neutral equilibrium position of the cross-bridge and the nearest actin site is x, whether or not the cross-bridge is actually bonded to that site. It is worth noting that various calcium activation mechanisms lead to the same form of generalized Huxley rate equation governing the actin-myosin bond-distribution function, i.e. to Eq. (3.1), if it is assumed that calcium binding dynamics are fast compared to the rate of cross-bridge transition to and from the force-generating states.

A different approach to modelling skeletal muscle contraction was used by NAKAMACHI *et al.* [57]. These authors exploited an idea primarily developed in [56]. This theory is based on three macromolecular potentials defined by a one-dimensional function along the sliding direction, cf. Fig. 4a. The periodic potential U_0 along the actin filament has the period of G-actin alignment. Simplifying the noncovalent bonding potential between myosin heads and actin filaments as a sinusoidal relationship we write

$$U_0(x) = \frac{H_0}{2}\left[\cos\left(\frac{2\pi x}{L}\right) - 1\right], \tag{3.2}$$

where x is the coordinate along the actin filament, L is the helix period of the actin filament (5.46 nm in frog skeletal muscle), and H_0 denotes the amplitude of this potential.

The self-induced potential U_i is generated by ATP hydrolysis, which is activated by the increasing concentration of ionized calcium emitted from the sarcoplasmic reticulum. This potential forces myosin heads to slide along the actin filament, causing muscle contraction and is assumed in the following form:

$$U_i = w(t)u(X), \tag{3.3}$$

where

$$w(t) = w_0 \exp(-k_1 t)[1 - \exp(-k_2 t)], \tag{3.4}$$

$$u(X) = \frac{1}{\sqrt{2\pi}\sigma} \exp\left(-\frac{X^2}{2\sigma^2}\right). \tag{3.5}$$

Here X denotes the coordinate of myosin heads, and σ is the standard deviation of normal distribution.

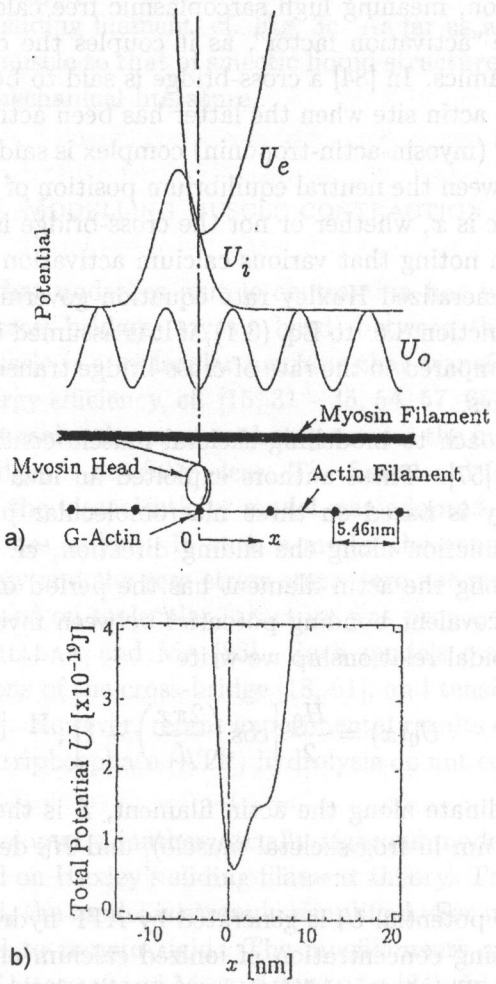

FIG. 4. Macromolecular potential theory, a) molecular potential model; b) total potential, after [57].

The elastic potential U_c is associated with heavy meromyosin. U_e works as the spring that transmits the force generated on the myosin heads by ATP hydrolysis to the thick myosin filament. The potential U_e was assumed in the form

$$U_e = \begin{cases} A_1\Delta l^2 + A_2\Delta l & \text{if} \quad \Delta l \geq 0, \\ A_3\Delta l^2 & \text{if} \quad \Delta l \leq 0, \end{cases} \tag{3.6}$$

where A_1, A_2 and A_3 are constants and Δl is the deviation from the zero tension position.

The total potential U on a myosin head is the sum of these three potentials:

$$U = U_0 + U_i + U_e. \tag{3.7}$$

NAKAMACHI *et al.* [57] also introduced an atomic potential energy to study the atomic mechanical properties of protein, which constitutes the skeletal muscle. The minimum conformation energy search was performed to find the 3D atomic structure under the defined conditions of the molecule and its environment.

In a series of papers [66 – 68], on the basis of available experimental data, a new model of actin-myosin interaction has been developed. In essence, this new approach uses computer modelling and simulation. However, mathematically rigorous analysis supporting this type of modelling is still lacking. Nevertheless, the simulation results are impressive. The main difference with more traditional approaches consists in assuming that the tail is arranged along a helical track and the configuration of three-cross bridges is not symmetrical as is conventionally assumed.

In muscle mechanics very famous is the following Hill's equation [19 – 22], cf. also FUNG [15],

$$(\nu + b)(P + a) = b(P_0 + a), \tag{3.8}$$

where P represents tension in a muscle, ν represents the velocity of contraction, and a, b, P_0 are constants. Equation (3.8) reveals only one aspect of the muscle behaviour, namely the ability of tetanized muscle to contract. It is an empirical equation based on experimental data on frog sartorius muscle. Hence the need for more comprehensive approach. Earlier attempts in this direction were critically reviewed by FUNG [15], cf. also [68]. Particularly, very popular is the Hill's three-element model [15]. This model represents an active muscle as composed by three elements. Two elements are arranged in series: (a) a contractile element, which at rest is freely extensible (i.e., it has zero tension), but when activated, it is capable of shortening; and (b) an elastic element arranged in series with the contractile element. To account for the elasticity of the muscle at rest, a "parallel elastic element" is added.

One of muscle characteristics is the three-dimensional relationship between muscle length, velocity and force. According to experimental data, muscle force is not a simple function of instantaneous length and velocity. Instead, muscle force also depends on how the muscle arrives at a certain length or velocity [54, 55]. A simple Hill-type model accounting for such interdependance has been proposed in [54, 55]. The parameters for contractile elements, involved in the model, were determined from experiments performed on in situ medical gastrocnemius muscle of 10 male Wistar rates.

An inspection of muscle contraction models reveals one specific feature: spatial effects of contractions usually neglected. More profound study was undertaken by VAN DONKELAAR [72] with respect to deformation and perfusion. More precisely, the three-dimensional deformations of skeletal muscle during contraction were determined. The second aim in [72] was to study the interaction between contraction and perfusion and to explore spatial effects that interfere with this interaction. VAN DONKELAAR'S study [72] is confined to the presentation of numerical results and some experimental data. Unfortunately, mathematical models were not given.

4. BASIC RELATIONS AND GENERAL FORM OF THE STORED ENERGY FUNCTION FOR ISOTROPIC HYPERELASTIC MATERIALS

As usual, by $\mathbf{F}$ we denote the deformation gradient and $\mathbf{C} = \mathbf{F}^T\mathbf{F}$ is the right Cauchy-Green strain tensor, cf. [7, 8, 10, 58]. We recall that $\mathbf{F}^T$ stands for the transpose of $\mathbf{F}$. We assume that $J = \det\mathbf{F} > 0$. The objectivity principle yields the stored energy function in the form [10, 58]

$$W = \breve{W}(\mathbf{C}). \tag{4.1}$$

Let us denote by $\mathbf{T}$, $\boldsymbol{\sigma}$ the second (symmetric) Piola-Kirchhoff and Cauchy stress tensors, respectively. We have

$$\mathbf{T} = \frac{\partial\breve{W}(\mathbf{C})}{\partial\mathbf{C}} + \frac{\partial\breve{W}(\mathbf{C})}{\partial\mathbf{C}^T}, \qquad \boldsymbol{\sigma} = \frac{1}{J}\mathbf{F}\mathbf{T}\mathbf{F}^T. \tag{4.2}$$

The first (unsymmetric) Piola-Kirchhoff stress tensor $\mathbf{S}$ is related to $\mathbf{T}$ by $\mathbf{S} = \mathbf{F}\mathbf{T}$.

For isotropic hyperelastic materials satisfies [10, 37, 58]

$$\breve{W}(\mathbf{C}) = \breve{W}(\mathbf{Q}\mathbf{C}\mathbf{Q}^T), \qquad \forall\mathbf{Q} \in O(3). \tag{4.3}$$

Here $O(3)$ denotes full orthogonal group in space dimension 3.

We assume the existence of a stress and strain-free state (natural configuration) such that

$$\breve{W}(\mathbf{I}) = 0, \qquad \mathbf{T} = \breve{\mathbf{T}}(\mathbf{I}) = \mathbf{0}, \tag{4.4}$$

where $\mathbf{I}$ is the idenity tensor.

By now it has been well-established that in many soft tissues residual stresses and strains are present [2, 12, 16] and Part II of our paper. Consequently, assumption $(4.4)_2$ for such tissues is, in a general case, a simplification. Fortunately, an isotropic body can support no residual stress [24]. Thus for an ideal case of isotropic soft tissues assumption (4.4) remains valid.

Having in mind FEM it is convenient to choose the invariants of $\mathbf{C}$ compatible with the multiplicative decomposition of $\mathbf{F}$ in parts related to volumetric and distortional deformations as well as with the polar decomposition, the last being expressed by the well-known relation $\mathbf{F} = \mathbf{RU} = \mathbf{VR}$. In this manner one can formulate in a uniform manner the constitutive relationships for compressible and incompressible materials. Accordingly, we write

$$\mathbf{F} = J^{1/3}\overline{\mathbf{F}} = J^{1/3}\mathbf{R}\overline{\mathbf{U}} = J^{1/3}\overline{\mathbf{V}}\mathbf{R}, \qquad \det\overline{\mathbf{F}} = \det\overline{\mathbf{U}} = \det\overline{\mathbf{V}} = 1. \tag{4.5}$$

Consequently, the stored energy function (4.1) satisfying (4.3) can be written as follows [37]

$$W = \breve{W}(\mathbf{C}) = \breve{W}(\mathbf{B}) = \overline{W}(\overline{I_1}, \overline{I_2}, J), \tag{4.6}$$

where

$$\overline{I_1} = \mathrm{tr}\overline{\mathbf{B}} = \mathrm{tr}\overline{\mathbf{C}}, \quad \overline{I_2} = \mathrm{tr}\overline{\mathbf{B}}^{-1} = \mathrm{tr}\overline{\mathbf{C}}^{-1}, \tag{4.7}$$

$$J = \sqrt{\det\mathbf{B}} = \sqrt{\det\mathbf{C}} = \det\mathbf{F}.$$

and

$$\mathbf{B} = \mathbf{F}\mathbf{F}^T, \qquad \overline{\mathbf{B}} = \overline{\mathbf{F}}\overline{\mathbf{F}}^T, \qquad \overline{\mathbf{C}} = \overline{\mathbf{F}}^T\overline{\mathbf{F}}. \tag{4.8}$$

We observe that

$$\overline{I_1} = J^{-\frac{2}{3}}I_1, \qquad I_1 = \mathrm{tr}\mathbf{C} = \mathrm{tr}\mathbf{B}, \qquad \overline{I_2} = J^{-\frac{4}{3}}I_2, \tag{4.9}$$

$$I_2 = \frac{1}{2}(I_1^2 - \mathrm{tr}\mathbf{C}^2), \qquad \mathrm{tr}\mathbf{C}^2 = \mathrm{tr}\mathbf{B}^2.$$

We also recall that the invariants I_1, I_2 and J^2 are the so-called basic invariants, well-known in the theory of tensor functions representation, cf. [37].

After standard calculations, from relationships (4.2) and (4.6) we get the general constitutive equation for isotropic hyperelastic materials in the Eulerian description

$$\boldsymbol{\sigma} = \frac{\partial \overline{W}}{\partial J}\mathbf{I} + \frac{2}{J}\left(\frac{\partial \overline{W}}{\partial \overline{I}_1}\overline{\mathbf{B}}_D - \frac{\partial \overline{W}}{\partial \overline{I}_2}\overline{\mathbf{B}}_D^{-1}\right) = \beta_0\mathbf{I} + \beta_1\overline{\mathbf{B}}_D + \beta_{-1}\overline{\mathbf{B}}_D^{-1}, \tag{4.10}$$

where

$$\overline{\mathbf{B}}_D = \overline{\mathbf{B}} - \frac{1}{3}\overline{I}_1\mathbf{I}, \qquad \overline{\mathbf{B}}_D^{-1} = \overline{\mathbf{B}}^{-1} - \frac{1}{3}\overline{I}_2\mathbf{I}. \tag{4.11}$$

The form $(4.6)_3$ of the stored energy function enables to classify hyperelastic isotropic materials as follows:

(i) incompressible materials $(J - 1 = 0)$ where

$$W = W_D(\overline{I}_1, \overline{I}_2), \tag{4.12}$$

(ii) nearly incompressible materials described by

$$W = W_D(\overline{I}_1, \overline{I}_2) + W_I(J), \tag{4.13}$$

(i) compressible materials described by the elastic potential $(4.6)_3$.

More precisely, the function W_I has the following form, cf. [10, 47],

$$W_I(J) = \frac{1}{3}h(\det\mathbf{F}).$$

The function h satisfies:

$$h : R^+ \to R \quad \text{is convex}, \tag{H_1}$$

$$\lim_{\delta\to 0^+} h(\delta) = \lim_{\delta\to+\infty} h(\delta) = +\infty, \quad \text{and} \quad h(\delta) = 0 \ \text{ if and only if } \ \delta = 1. \tag{H_2}$$

Obviously, in the case of incompressible materials the stored energy function (4.12) *is not an elastic potential*, since the hydrostatic part of the Cauchy stress tensor is not defined and the constitutive relationship is given by

$$\boldsymbol{\sigma} = -p\mathbf{I} + \overline{\beta}_1\overline{\mathbf{B}} + \overline{\beta}_{-1}\overline{\mathbf{B}}^{-1}, \tag{4.14}$$

where

$$\overline{\beta}_1 = 2\frac{\partial W_D}{\partial \overline{I}_1}, \qquad \overline{\beta}_{-1} = -2\frac{\partial W_D}{\partial \overline{I}_2}. \tag{4.15}$$

The above classification is convenient when FEM ABAQUS [1] is used as in our case. Obviously, in the case of incompressible materials the coupling between distorsional and volumetric stored energies is absent.

Let us denote by λ_i, $\overline{\lambda}_i$ $(i = 1, 2, 3)$ the eigenvalues of $\mathbf{U}$ and $\overline{\mathbf{U}}$ respectively, or of $\mathbf{V}$ and $\overline{\mathbf{V}}$. We have

$$\lambda_i = J^{1/3}\overline{\lambda}_i; \qquad i = 1, 2, 3. \tag{4.16}$$

In general, only two eigenvalues of $\overline{\lambda}_i$ are independent. We may write

$$\overline{\lambda}_3 = \left(\overline{\lambda}_1 \overline{\lambda}_2\right)^{-1}. \tag{4.17}$$

Consequently, we have, cf. Eq. (4.6),

$$\overline{W}(\overline{I}_1, \overline{I}_2, J) = \hat{W}(\overline{\lambda}_1, \overline{\lambda}_2, J). \tag{4.18}$$

The function $\hat{W}$ is symmetric in the variables $\overline{\lambda}_1, \overline{\lambda}_2$. For the notion of symmetric function in the context of nonlinear hyperelasticity the reader is referred to [10].

5. Stored energy functions for isotropic hyperelastic soft tissue

The aim of this section is to provide several specific stored energy functions as well as numerical examples.

5.1. General developments

Let us consider the following stored energy function, being a generalisation of Fung's proposal [15]

$$W\left(\overline{I}_1, \overline{I}_2, J\right) = \frac{C}{a}\left(e^{a\psi(\overline{I}_1, \overline{I}_2, J)} - 1\right), \tag{5.1}$$

where C and a are material coefficients while the invariants $\overline{I}_1, \overline{I}_2$ and J have been defined in the previous section. Now the Cauchy's stress tensor is expressed by $(4.10)_2$ and

$$\beta_0 = Ce^{a\psi}\frac{\partial \psi}{\partial J}, \qquad \beta_1 = \frac{2}{J}Ce^{a\psi}\frac{\partial \psi}{\partial \overline{I}_1}, \qquad \beta_{-1} = -\frac{2}{J}Ce^{a\psi}\frac{\partial \psi}{\partial \overline{I}_2}. \tag{5.2}$$

According to relation (4.4), we assume

$$\psi(3, 3, 1) = 0, \qquad \mathbf{T} = \tilde{\mathbf{T}}(\mathbf{I}) = \mathbf{0}. \tag{5.3}$$

In other words, in the undeformed configuration the hyperelastic solid is stress-free. The function appearing in Eq. (5.1) has one of the following forms

(a) $$\psi = \psi(\overline{I}_1, \overline{I}_2),$$

(b) $$\psi = \psi_1(\overline{I}_1, \overline{I}_2) + \psi_2(J),$$

(c) $$\psi = \psi_1(\overline{I}_1, \overline{I}_2, J).$$

It is reasonable to consider the following form of ψ:

$$\psi = a_1(\overline{I}_1 - 3) + a_2(\overline{I}_2 - 3) + a_3(J-1) + a_4\overline{I}_1\overline{I}_2 - 9) + ..., \tag{5.4}$$

where the parameters are material coefficients.

In the present section we will discuss only the models (a) and (c) of soft tissues. For such models the material parameters are known. Also, an implementation in the finite element programme ABAQUS will be discussed.

In the case of incompressible materials the following particular form of the function (5.1), now denoted by W, is assumed:

$$W(\overline{I}_1) = \frac{\mu_0}{2\gamma}\left[e^{\gamma(\overline{I}_1-3)} - 1\right], \tag{5.5}$$

where μ_0 denotes the shear modulus and γ is a positive material parameter.

For compressible materials we consider the following stored energy function

$$W(\overline{I}_1, \overline{I}_2, J) = \frac{C_0}{2}\left[e^{C_1(\overline{I}_1-3)+C_2(\overline{I}_2-3)+C_3(J-1)^2} - 1\right], \tag{5.6}$$

where $C_0, C_i (i = 1,2,3)$ are positive material parameters, see [64, 65].

We observe that material parameters appearing in Eqs. (5.5), (5.6), and more generally in (5.4), can be determined by performing simple tests (one- and two-dimensional) and next by minimizing the approximation error (similarly to the case of other hyperelastic materials, cf. [58]).

Also, function (5.5) is a particular case of (5.6). However, from the numerical and mechanical point of view it is convenient to treat both models as independent. For the sake of simplicity, models (5.5) and (5.6) will be denoted by IM and CM, respectively.

In the case of the model IM the constitutive relationship is given by

$$\boldsymbol{\sigma} = -p\mathbf{I} + \mu_0 e^{\gamma(\overline{I}_1-3)}\overline{\mathbf{B}}. \tag{5.7}$$

For three-dimensional and plane strain problem, an application of FEM to incompressible materials requires hybrid finite elements (or a modification of models (a) and (b)).

For the plane stress problem the situation is different, since then the incompressibility constraint can easily be handled. We observe that for incompressible

material in the state of plane stress, the stretch in the direction orthogonal to the plane is determined from the equation $J = 1$; hence

$$\lambda_3 = \tilde{J}^{-1}. \tag{5.8}$$

Here the tilde refers to two-dimensional quantities. It means that $\tilde{J}$ denotes the determinant of plane deformation tensor. From Eq. (5.7), for the plane stress state, we have

$$p = \mu_0 e^{\gamma(\tilde{I}+\tilde{J}^{-2}-3)}\tilde{J}^{-2}. \tag{5.9}$$

Thus

$$\tilde{\sigma} = \mu_0 e^{\gamma(\tilde{I}+\tilde{J}^{-2}-3)}\left(-\tilde{J}^{-2}\tilde{\mathbf{I}} + \tilde{\mathbf{B}}\right). \tag{5.10}$$

where $\tilde{I} = \mathrm{tr}\tilde{\mathbf{B}} = \mathrm{tr}\tilde{\mathbf{C}}$.

The derivation of the constitutive relationship in the case of the stored energy function (5.6) is left to the reader as an easy exercise.

5.2. Implementation of IM and CM models in the programme ABAQUS

The model IM requires programming, within the general structure of the interface UHYPER (see [36]), of only the first- and second-order derivatives with respect to the invariant $\bar{I}_1$ of the function (5.5). On the other hand, in the FORTRAN code the model CM requires programming of the following derivatives of the function (5.6):

$$\begin{aligned}
&\frac{\partial W}{\partial \bar{I}_1} = \frac{1}{2}C_0C_1e^{\phi}, \qquad \frac{\partial W}{\partial \bar{I}_2} = \frac{1}{2}C_0C_2e^{\phi}, \qquad \frac{\partial W}{\partial J} = \frac{1}{2}C_0C_3e^{\phi}(J-1),\\
&\frac{\partial^2 W}{\partial \bar{I}_1^2} = \frac{1}{2}C_0C_1^2e^{\phi}, \qquad \frac{\partial^2 W}{\partial \bar{I}_2^2} = \frac{1}{2}C_0C_2^2e^{\phi},\\
&\frac{\partial^2 W}{\partial J_2} = C_0C_3e^{\phi}\left[1+2C_3(J-1)^2\right], \qquad \frac{\partial^2 W}{\partial \bar{I}_1\partial \bar{I}_2} = \frac{1}{2}C_0C_1C_2e^{\phi},\\
&\frac{\partial^2 W}{\partial \bar{I}_1\partial J} = C_0C_1C_3e^{\phi}(J-1), \qquad \frac{\partial^2 W}{\partial \bar{I}_2\partial J} = C_0C_2C_3e^{\phi}(J-1),\\
&\frac{\partial^3 W}{\partial \bar{I}_1^2\partial J} = C_0C_1^2C_3e^{\phi}(J-1), \qquad \frac{\partial^3 W}{\partial \bar{I}_2^2\partial J} = C_0C_2^2C_3e^{\phi}(J-1),\\
&\frac{\partial^3 W}{\partial \bar{I}_1\partial \bar{I}_2\partial J} = C_0C_1C_2C_3e^{\phi}(J-1),
\end{aligned} \tag{5.11}$$

(5.11) [cont.]
$$\frac{\partial^3 W}{\partial \bar{I}_1 \partial J^2} = C_0 C_1 C_3 e^{\phi}[1 + 2C_3(J-1)^2],$$

$$\frac{\partial^3 W}{\partial \bar{I}_2 \partial J^2} = C_0 C_2 C_3 e^{\phi}[1 + 2C_3(J-1)^2],$$

$$\frac{\partial^3 W}{\partial J^3} = 2C_0 C_3^2 e^{\phi}[3 + 2C_3(J-1)^2](J-1),$$

where

(5.12)
$$\phi = C_1(\bar{I}_1 - 3) + C_2(\bar{I}_2 - 3) + C_3(J-1)^2.$$

5.3. Numerical examples: model IM

The aim of this section is to provide illustrative example for the IM model. We observe that, in general, it is more difficult to obtain satisfactory numerical results for this model than for the CM model. As one can guess, the difficulty is linked with the incompressibility condition.

EXAMPLE 5.1. *Simple shear (plane stress problem)*

Now we have

$$\sigma_{11} = \mu_0 \xi^2 e^{\gamma \xi^2}, \qquad \sigma_{22} = 0, \qquad \sigma_{12} = \mu_0 \xi e^{\gamma \xi^2}, \qquad \sigma_{33} = \sigma_{13} = \sigma_{23} = 0.$$

For the notation the reader is referred to Fig. 5. Figure 6 represents a comparison of analytical and numerical results. The last one has been obtained by using interface UHYPER with the implemented IM model. Both the Poynting effect (nonvanishing normal stress) and Kelvin effect (nonvanishing trace of the stress tensor) are exhibited. The results presented in Fig. 6 are valid provided that the state of simple shear is realized. This can be achieved if simultaneously the di-

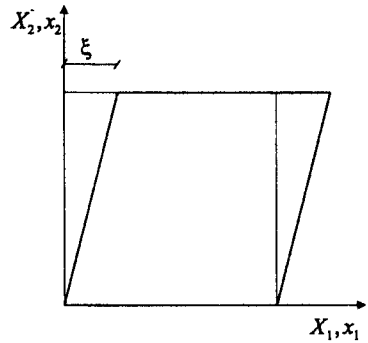

FIG. 5. Simple shear.

splacements and forces on the boundaries are controlled. Otherwise, the situation depicted in Fig. 7 may happen. For instance, in Fig. 7a, only the displacements on the upper boundary are controlled.

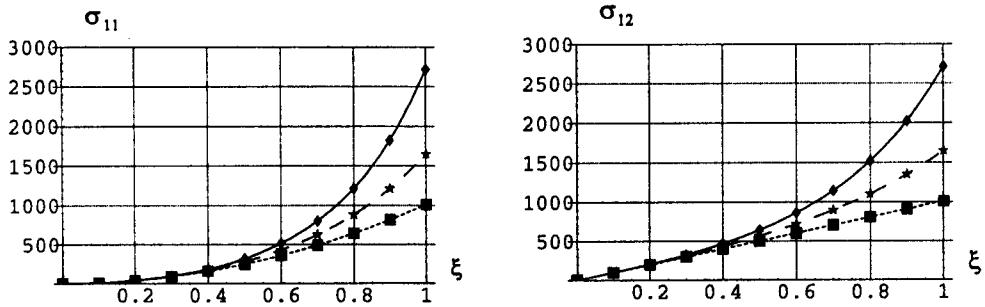

FIG. 6. Comparison of analytical and numerical results for simple shear (plane stress state); $\mu_0 = 1000$; the coefficient γ for the curves 1, 2, 3 is equal to: $\gamma = 1$, $\gamma = 0.5$, $\gamma = 0.01$.

EXAMPLE 5.2. *Thick cylinder subject to internal pressure (plane stress)*

The internal and external radii of cylinder in Fig. 8 are equal to $R_i = 10$ and $R_0 = 20$ (length units), respectively. The cylinder is subject to such an internal pressure that its boundary undergoes the displacement equal to 5 length units. The results of calculation are depicted in Figs. 9, 10.

5.4. Numerical examples: model CM

The results which follow have been performed for the following values of coefficients: $C_0 = 8133$ N/m^2, $C_1 = 0.907$, $C_2 = 0.002475$, $C_3 = 20$. These values are taken from paper [65] and characterize a rabbit aorta.

EXAMPLE 5.3. *Simple shear (plane strain or 3D problem)*

In this case, from Eqs. (5.2) and (5.6) we get

$$\sigma_{11} = C_0 e^{\xi^2(C_1+C_2)} \left[\frac{1}{3}\xi^2(2C_1 + C_2)\right],$$

$$\sigma_{12} = C_0 e^{\xi^2(C_1+C_2)}(C_1 + C_2)\xi,$$

$$\sigma_{22} = C_0 e^{\xi^2(C_1+C_2)} \left[-\frac{1}{3}\xi^2(C_1 + 2C_2)\right],$$

$$\sigma_{33} = C_0 e^{\xi^2(C_1+C_2)} \left[-\frac{1}{3}\xi^2(C_1 - C_2)\right].$$

The results of calculation are depicted in Fig. 11. Numerical calculations were

performed by using the interface UHYPER with the model CM implemented according to Eqs. (5.11), (5.12).

a)

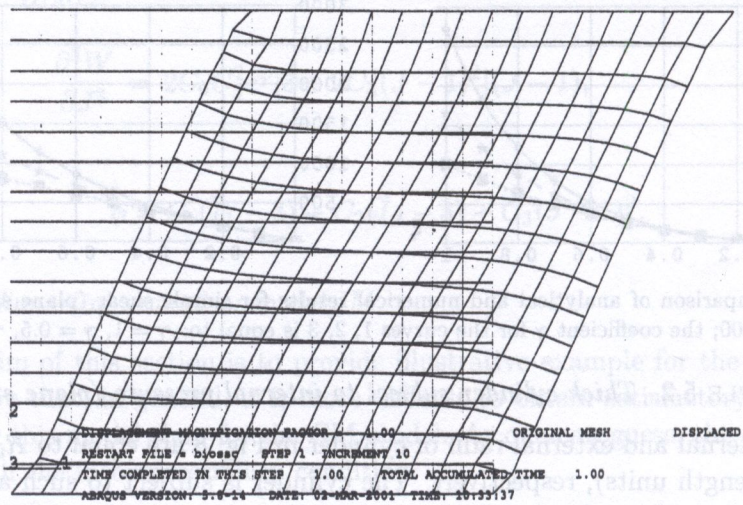

b)

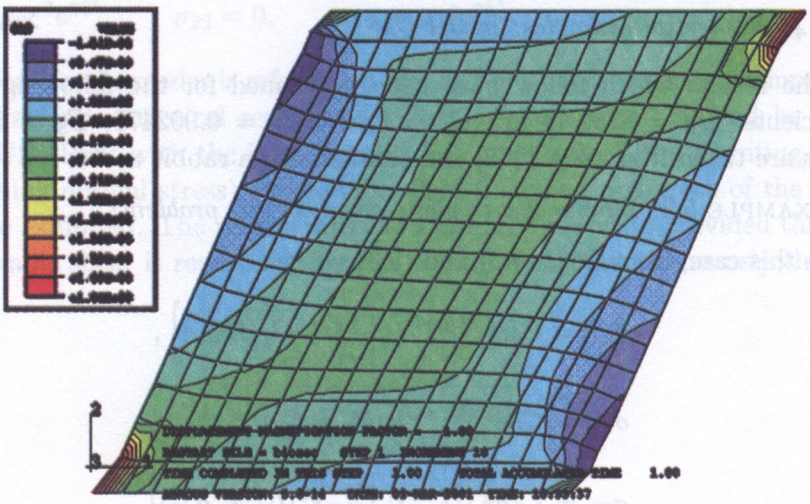

FIG. 7. Shear: a) FEM mesh and the final configuration; b) level lines for the Cauchy stress σ_{12}; $\mu_0 = 10^6$, $\gamma = 1$.

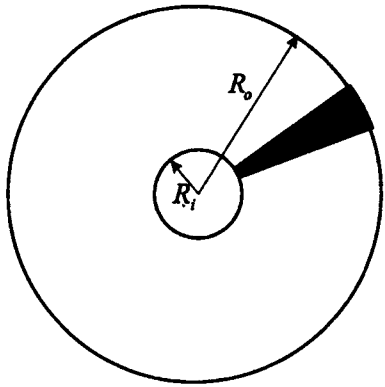

FIG. 8.

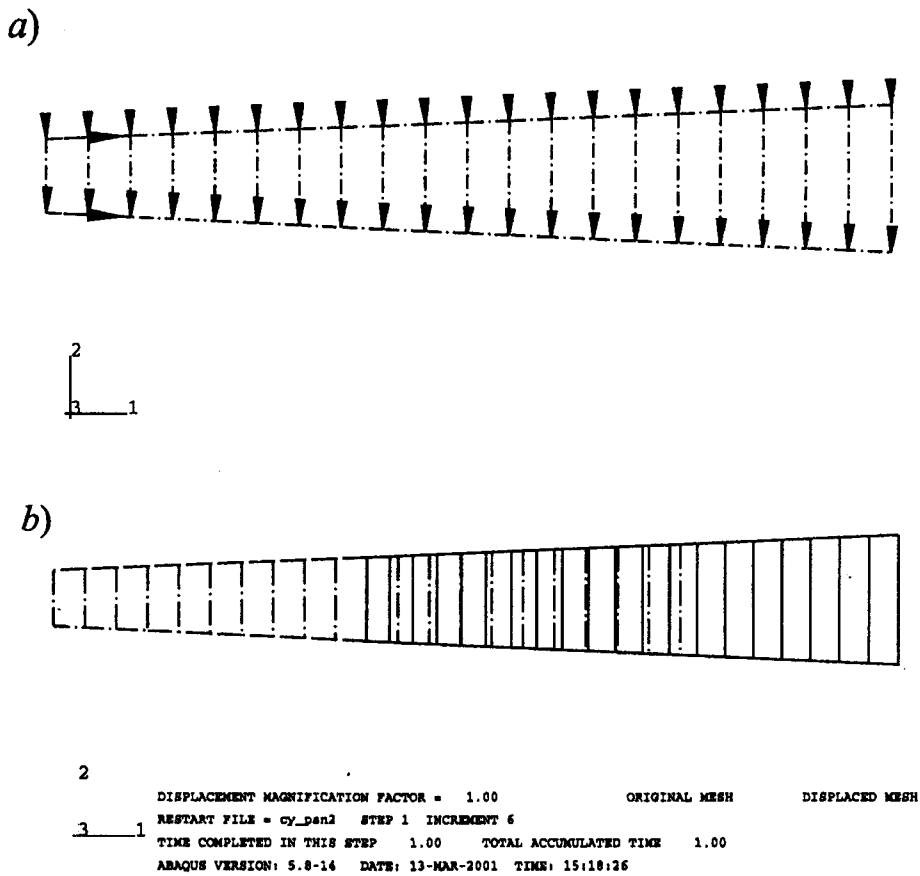

FIG. 9. Thick cylinder in plane stress state: a) FEM mesh and boundary condition; b) initial and final configurations.

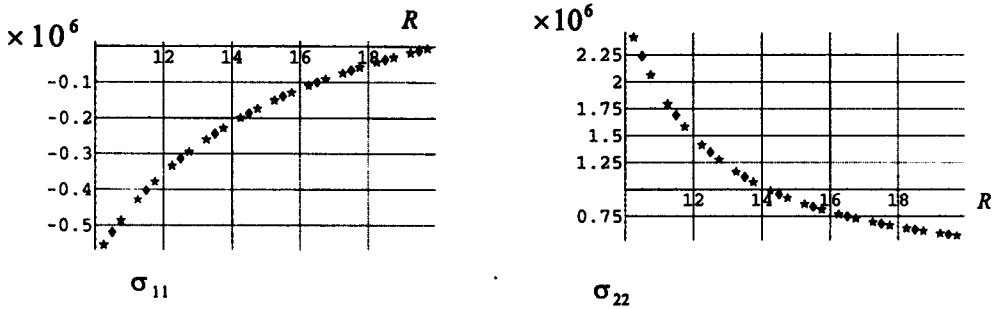

FIG. 10. Thick cylinder in plane stress state (10 or 20 finite elements); $\mu_0 = 10^6$, $\gamma = 1$. Cauchy's stresses σ_{11} and σ_{22} represent values averaged (centrally) over the finite elements.

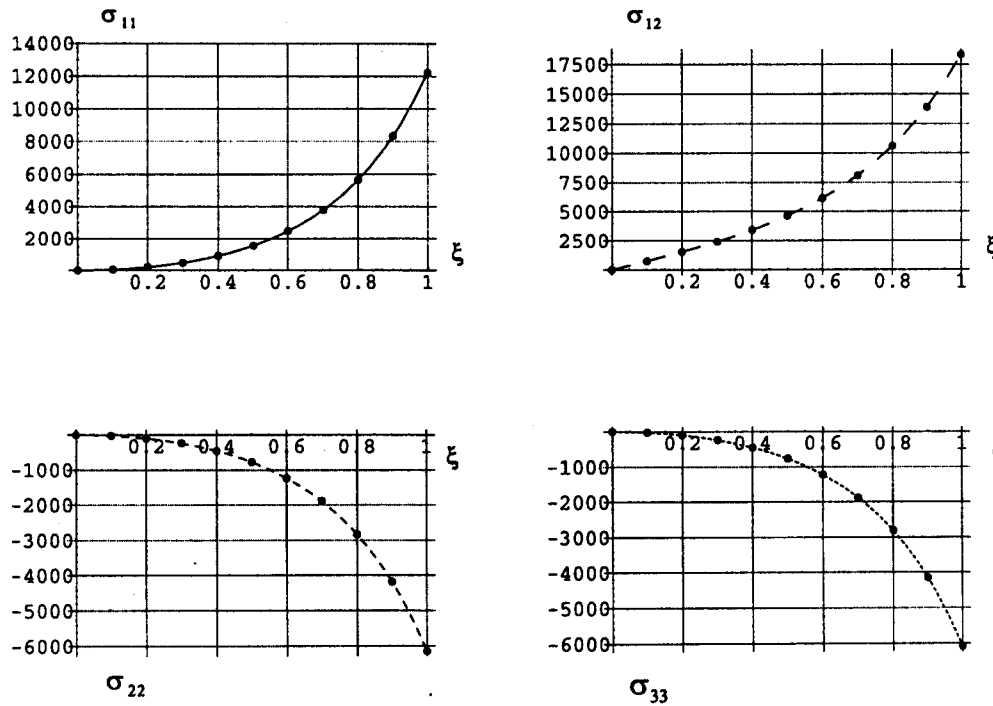

FIG. 11. Comparison of analytical and numerical results for simple shear (plane strain state or 3D problem).

EXAMPLE 5.4.

Consider now the slab with a central hole with the unit thickness. The length of the side of the square is 2 length units. The diameter of the hole is 0.2 length units. The slab is subject to tension in one direction such that its length increases fivefolds, see Fig. 12. The vertical displacement on AB and CD is constrained. To get the numerical results, the slab was divided into 512 finite elements CPS4. The results presented in Fig. 12 were obtained after 15 iterations.

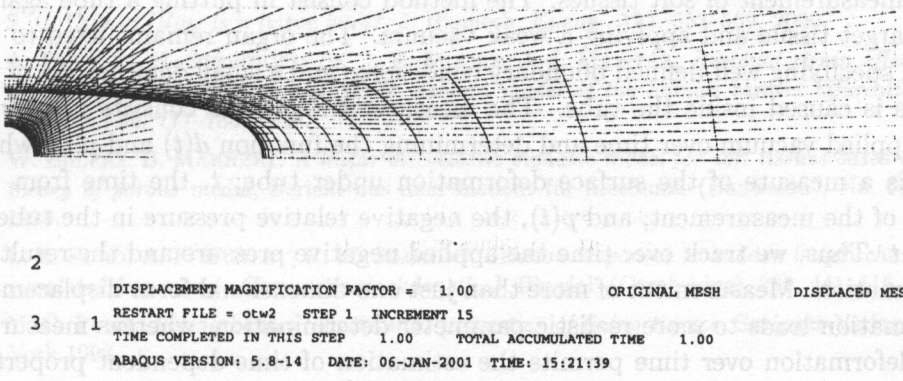

FIG. 12. The initial and final configurations of square slab with a hole.

6. FINAL REMARKS

We have proposed several constitutive equations applicable to isotropic soft tissues. Isotropy may be an acceptable assumption even for anisotropic tissues. For instance, VAN KEMENADE [41] used the triphasic mixture theory for skin. The three components are the solid, fluid and ionic phases. The solid phase was treated as an isotropic Saint-Venant Kirchhoff material, though the skin exhibits anisotropic behaviour, cf. [15]. ATKINSON [4] studied the skin stretched by the silastic implant.

In order to simulate the eye response, JOUVE [40] also used the Saint-Venant Kirchhoff model. This author also applied simple transversely isotropic models. YEH *et al.* [82] developed a closed shell structured eyeball model for radial keratotomy. The analysis of corneal collagen laminae required for the tissue to be transversely isotropic. The cornea, as well as the limbus and sclera, was considered as homogeneous and isotropic. Only small displacements were considered in the implementation.

HUMPHREY [26] reviewed biomechanical modelling of biological membranes via a continuum membrane theory, cf. also [29]. There are many different mem-

branes within the human body, including aneurysms which form in the vasculature, cell membranes, the mesentery, the meninges which envelope the brain and spinal chord, the pericardia which surround the heart, the pleura which covers the lungs, skin, the urinary bladder, etc. The biomembranes have usually been viewed as hyperelastic and possibly anisotropic membranes.

Some experimental procedures devised for testing soft tissues will be presented in Part II, cf. also [75] and the references therein. Here we only mention the paper by VUSKOVIC *et al.* [76]. These authors described the method for in-vivo measurement of soft tissues. The method consist in putting a tube against the target tissue and applying a weak vacuum. The organ remains fixed to the tube, specifying well-defined boundary conditions, and a small deformation of the tissue is caused inside the tube. The measurement process consists in varying the applied vacuum over time and determining the function $d(t)$ and $p(t)$, where $d(t)$ is a measure of the surface deformation under tube; t, the time from the start of the measurement; and $p(t)$, the negative relative pressure in the tube at time t. Thus, we track over time the applied negative pressure and the resulting deformation. Measurement of more than just one-dimensional force-displacement information leads to more realistic parameter determination, whereas measuring the deformation over time permits the estimation of time-dependent properties such as viscoelasticity.

ACKNOWLEDGEMENT

The authors were supported by the State Committee for Scientific Research (KBN, Poland) through the grant No. 8 T11F 017 18.

REFERENCES

1. ABAQUS, *Theory manual*, Version 5.7; ABAQUS/Standard *Example problems manual*, Version 5.7; ABAQUS/Standard *User's manual*, Version 5.7; ABAQUS/Standard *Verification manual*, Version 5.7., Hibbitt, Karlsson and Sorensen, Inc., Pawtucket, 1997.
2. T. ADACHI, M. TANAKA, Y. TOMITA, *Uniform stress state in bone structure with residual stress*, J. Biomech. Engng., **120**, 342–347, 1998.
3. M.-G. ASCENZI, *A first estimation of prestress in so-called circularly fibered osteonic lamellae*, J. Biomech., **32**, 935–942, 1999.
4. C. ATKINSON, *On a possible theory for the design of tissue expanders*, Quart. J. Mech. Appl. Math., **41**, 301–317, 1988.
5. T. S. ATKINSON, R. C. HAUT, N. J. ALTIERO, *A poroelastic model that predicts some phenomenological responses of ligaments and tendons*, J. Biomech. Engng., **119**, 400–405, 1997.

6. M. F. BEATTY, *Topics in finite elasticity: Hyperelasticity of rubber, elastomers, and biological tissues-with examples*, Appl. Mech. Reviews, **40**, Part 1, 1699–1734, 1987.

7. M. F. BEATTY, *Introduction to nonlinear elasticity*, [In:] *Nonlinear effects in fluids and solids*, M. M. CARROLL and M. HAYES [Eds.], Plenum Press, 13–112, New York 1996.

8. J. BONET, R. D. WOOD, *Nonlinear continuum mechanics for finite element analysis*, Cambridge University Press, Cambridge 1997.

9. G. H. BROWN, J. J. WOLKEN, *Liquid crystal and biological structures*, Academic Press, New York 1979.

10. P. G. CIARLET, *Mathematical elasticity*, North-Holland, Amsterdam 1988.

11. S. C. COWIN, *How is a tissue built?*, J. Biomech. Engng., **122**, 553–569, 2000.

12. A. DELFINO, N. STERGIOPULOS, J. E. MOORE, J.-J. MEISTER, *Residual strain effects on the stress field in a thick wall finite element model of the human carotid bifurcation*, J. Biomech., **30**, 777–786, 1997.

13. W. EHLERS, B. MARKERT, *A linear viscoelastic biphasic model for soft tissues based on the theory of porous media*, Bericht aus dem Institut für Mechanik (Bauwesen), No. 99-II-3, 1999.

14. L. E. FORD, A. F. HUXLEY, R. M. SIMMONS, *Tension responses to sudden length change in simulated frog muscle fibers near slack length*, J. Physiol. (Cambridge), **269**, 441–515, 1977.

15. Y. C. FUNG, *Biomechanics: mechanical properties of living tissues*, Springer-Verlag, New York 1993.

16. Y. C. FUNG, *Biomechanics: circulation*, Springer-Verlag, New York 1997.

17. L. GLASS, P. HUNTER, A. MCCULLOCH [Eds.], *Theory of heart*, Springer-Verlag, New York 1991.

18. J. E. HEUSER, R. COOKE, *Actin-myosin interactions visualized by the quick-freeze, deep-etch replica technique*, J. Mol. Biology, **169**, 97–122, 1983.

19. A. V. HILL, *The heat shortening and the dynamic constants of muscle*, Proc. R. Soc. London, Ser. B. Biol. Sci., **126**, 136–195, 1938.

20. A. V. HILL, *The energetics of relaxation in a muscle twitch*, Proc. R. Soc. London, Ser. B. Biol. Sci., **136**, 211–219, 1949.

21. A. V. HILL, *The instantaneous elasticity of active muscle*, Proc. R. Soc. London, Ser. B. Biol. Sci., **141**, 161–178, 1953.

22. D. K. HILL, *Tension due to interaction between the sliding filaments in resting striated muscle, the effect of simulation*, J. Physiology, **155**, 657–684, 1968.

23. A. HOFFMAN, *Determining the material properties of soft tissues*, Preprint, Mechanical Engineering Department, Worcester Polytechnic Institute, 1998.

24. A. HOGER, *On the residual stress possible in an elastic body with material symmetry*, Arch. Rat. Mech. Anal., **88**, 271–289, 1985.

25. G. A. HOLZAPFEL, *Biomechanics of soft tissues*, [In:] Handbook of material behaviour: nonlinear models and properties, J. LEMAITRE [Ed.], Academic Press, (in press).

26. J. D. HUMPHREY, *Computer methods in membrane biomechanics*, Comp. Meth. Biomech. Biomed. Engng., **1**, 171–210, 1998.

27. J. D. HUMPHREY, F. C. P. YIN, *A new constitutive formulation for characterizing the mechanical behavior of soft tissue*, Biophys. J., **52**, 563–570, 1987.

28. J. D. HUMPHREY, R. K. STRUMPF, F. C. P. YIN, *Determination of a constitutive relation for passive myocardium: I. A new functional form*, J. Biomech. Engng., **112**, 333–339, 1990; II. Parameter estimation, ibid., pp. 340–346.

29. J. D. HUMPHREY, R. K. STRUMPF, F. C. P. YIN, *A constitutive theory for biomembranes: application to epicardial mechanics*, J. Biomech., **114**, 461–466, 1992.

30. C. HURSCHLER, B. LOITZ-RAMAGE, R. VANDERBY, *A structurally based stress-stretch relationship for tendon and ligament*, J. Biomech. Engng., **119**, 392–399, 1997.

31. A. F. HUXLEY, *Muscle structure and theories of contraction*, Prog. Biophys. Biophys. Chem., **7**, 255–318, 1957.

32. H. E. HUXLEY, *The crossbridge mechanism of muscle contraction and its implications*, J. Exp. Biology, **115**, 17–30, 1985.

33. H. E. HUXLEY, J. HANSON, *Changes in cross-striations of muscle during contraction and stretch and their structural interpretation*, Nature, **173**, 973–976, 1954.

34. A. F. HUXLEY, R. NIEDERGERKE, *Interference microscopy of living muscle fibers*, Nature, **173**, 971–973, 1954.

35. A. F. HUXLEY, R. M. SIMONS, *Proposed mechanism of force generation in striated muscle*, Nature, **233**, 533–538, 1971.

36. S. JEMIOŁO, A. SZWED, *Implementation of subroutine UHYPER of ABAQUS finite element program for hyperelastic Blatz-Ko material*, [In:] Theoretical Foundations of Civil Engineering, W. SZCZEŚNIAK [Ed.], ZG OW PW, 251–262, Warsaw 1999.

37. S. JEMIOŁO, J. J. TELEGA, *Representations of tensor functions and applications in continuum mechanics*, IFTR Reports, 3/1997, Warsaw.

38. S. JEMIOŁO, J. J. TELEGA, *Implementation of isotropic hyperelastic models of soft biological tissues in finite element program ABAQUS*, [In:] Theoretical Foundations of Civil Engineering, W. SZCZEŚNIAK [Ed.], ZG OW PW, 269–280, Warsaw 1999.

39. S. JEMIOŁO, J. J. TELEGA, *Isotropic models of hyperelastic soft tissues: implementation in FEM ABAQUS*, Acta Bioeng. Biomech., **1**, Supplement 1, 207–210, 1999.

40. F. JOUVE, *Modélisation de l'œil en élasticité non linéaire*, Masson, Paris 1993.

41. P. VAN KEMENADE, *Water and ion transport through intact and damaged skin*, Ph. D. thesis, Technische Universiteit Eindhoven 1998.

42. P. KOWALCZYK, *Numerical analysis of stress distribution in lung parenchyma when interaction between tissue matrix and flowing air is taken into account* [in Polish], IFTR Reports 1/1993, Warsaw.

43. R. S. LAKES, R. VANDERBY, *Interrelation of creep and relaxation: a modelling approach for ligaments*, J. Biomech. Engng., **121**, 612–615, 1999.

44. Y. LANIR, *Constitutive equations for fibrous connective tissue*, J. Biomech., **16**, 1–12, 1983.

45. Y. LANIR, *Constitutive equations for the lung tissue*, J. Biomech. Engng., **105**, 374–380, 1983.

46. G. LAMM, A. SZABO, *Langevin nodes of macromolecules*, J. Chem. Phys., **85**, 7334–7348, 1986.

47. P. LE TALLEC, *Numerical methods for nonlinear three-dimensional elasticity*, [In:] Handbook of numerical analysis, P. G. CIARLET and J. L. LIONS [Eds.], Elsevier Science, Vol. III, 465–622, Amsterdam 1994.

48. G. C. LEE, *Solid mechanics of lungs*, J. Engng. Mech. Div., **104**, 177–199, 1978.

49. G. LEWIS, K. M. SHAW, *Modelling the tensile behavior of human Achilles tendon*, Bio-Medical Mat. Engng., **7**, 231–244, 1997.

50. D. H. S. LIN, F. C. P. YIN, *A multiaxial constitutive law for mammalian left ventricular myocardium in steady-state barium contracture in tetanus*, J. Biomech. Engng., **120**, 504–517, 1998.

51. J.-T. LIU, G. C. LEE, *Static finite deformation analysis of the lung*, J. Engng. Mech. Div., **104**, 225–238, 1978.

52. W. MAUREL, W. YIN, N. M. THALMAN, D. THALMAN, *Biomechanical models for soft tissues simulation*, Springer-Verlag, Berlin 1998.

53. K. MAY-NEWMAN, F. C. P. YIN, *A constitutive law for mitral valve tissue*, J. Biomech. Engng., **120**, 38–47, 1998.

54. K. MEIJER, *Muscle mechanics: the effect of stretch and shortening on skeletal muscle force*, P.D. thesis, Universiteit Twente, 1998.

55. K. MEIJER, H. J. GROOTENBOER, H. F. J. M. KOOPMAN, B. J. J. J. van der LINDEN, P. A. HUIJING, *A Hill type model of rat medial gastrocnemius muscle that accounts for shortening history effects*, J. Biomech., **31**, 555–563, 1998.

56. T. MITSUI, H. OSHIMA, *A self-induced translation model of myosin head motion in contracting muscle. I. Force-velocity relation and energy liberation*, J. Muscle Res. Cell Motil., **9**, 52–62, 1988.

57. E. NAKAMACHI, J. TSUKAMOTO, Y. TAMURA, *Molecular dynamics simulation of skeletal muscle contraction*, [In:] Computational Biomechanics, K. HAYASHI and H. ISHIKAWA [Eds.], Springer-Verlag, 89–114, Tokyo 1976.

58. R. W. OGDEN, *Nonlinear elastic deformations*, Ellis Horwood, Chichester 1984.

59. J. M. PRICE, *Biomechanics of smooth muscle*, [In:] Frontiers in biomechanics, G. W. SCHMID-SCHÖNBEIN, S. L.-Y. WOO and B. W. ZWEIFACH [Eds.], Springer-Verlag, 51–61, New York 1986.

60. M. A. PUSO, J. A. WEISS, *Finite element implementation of anisotropic quasi-linear viscoelasticity using a discrete spectrum approximation*, J. Biomech. Engng., **120**, 62–70, 1998.

61. M. K. REEDY, R. C. HOLMES, R. T. TREGEAR, *Induced changes in orientation of the cross-bridges of glycerinated insect flight muscle*, Nature, **207**, 1276–1281, 1965.

62. M. RENARDY, D. L. RUSSELL, *Formability of linear elastic structures with volume-type actuation*, Arch. Rat. Mech. Anal., **149**, 97–122, 1999.

63. B. R. SIMON, *Multiphase poroelastic finite element models for soft tissue structures*, Appl. Mech. Rev., **45**, 191–218, 1992.

64. B. R. SIMON, M. V. KAUFMAN, M. A. MCAFEE, A. L. BALDWIN, *Porohyperelastic finite element analysis of large arteries using ABAQUS*, J. Biomech. Engng., **120**, 296–298, 1998.

65. B. R. SIMON, M. V. KAUFMAN, M. A. MCAFEE, A. L. BALDWIN, L. M. WILSON, *Identification and determination of material properties for porohyperelastic analysis of large arteries*, J. Biom. Engng., **120**, 188–194, 1998.

66. L. SKUBISZAK, *Mechanism of muscle contraction*, Technol. Health Care, **1**, 133–142, 1993.

67. L. SKUBISZAK, L. KOWALCZYK, *Computer system modelling muscle work*, Technol. Health Care, **6**, 139–149, 1998.

68. L. SKUBISZAK, L. KOWALCZYK, *Relation between the mechanical properties of muscles and their structure on the molecular level*, Engng. Trans., **49**, 2–3, 191–212, 2001.

69. P. TONG, Y. C. FUNG, *The stress-strain relationship for the skin*, J. Biomech., **9**, 649–657, 1976.

70. A. TORELLI, *Study of a mathematical model for muscle contraction with deformable elements*, Rend. Sem. Mat. Univ. Pol. Torino, **55**, 241–271, 1997.

71. T. Q. P. UYEDA, H. M. WARRICK, S. J. KRON, J. A. SPUDICH, *Quantized velocities at low myosin densities in an in vitro motility assay*, Nature, **352**, 307–311, 1991.

72. C. C. VAN DONKELAAR, *Skeletal muscle mechanics: a numerical and experimental approach to spatial phenomena*, Universiteit Maastricht, 1999.

73. P. VENA, R. CONTRO, R. PIETRABISSA, L. AMBROSIO, *Design of materials subject to biomechanical compatibility constraints*, [In:] Synthesis in bio-solid mechanics, P. PEDERSEN and M. P. BENDSØE [Eds.], Kluwer Academic Publ., 67–78, Dordrecht 1999.

74. D. V. VORP, D. H.-J. WANG, *Use of finite elasticity in abdominal aneurysm research*, [In:] Mechanics in biology, J. CASEY and G. BAO [Eds.], 157–171, AMD - vo.242, The American Society of Mechanical Engineers, New York 2000.

75. J. VOSSOUGHI, A. TÖZEREN, *Determination of an effective shear modulus of aorta*, Russian J. Biomech., No 1-2, 20–35, 1998.

76. V. VUSKOVIĆ, M. KAMER, J. DUAL, M. BAJKA, *Method and device for in-vivo measurement of elasto-mechanical properties of soft biological tissues*, Machine Graphics Vision, **8**, 637–654, 1999.

77. H. W. WEIZSÄCKER, J. G. PINTO, *Isotropy and anisotropy of the arterial wall*, J. Biomech., **21**, 477–487, 1988.

78. S. L.-Y. WOO, J. S. WAYNE, *Mechanics of the anterior cruciate ligament and its contribution to knee kinematics*, Appl. Mech. Reviews, **43**, Part 2, 142–149, 1990.

79. S. L.-Y. WOO, G. A. JOHNSON, R. E. LEVINE, K. R. RAJAGOPAL, *Viscoelastic models for ligaments end tendons*, Appl. Mech. Reviews, **47**, Part 2, 282–286.

80. H. YAMADA, *Strength of biological materials*, The Williams & Wilkins Company, Baltimore 1970.

81. T. YANAGIDA, T. ARATA, F. OOSAWA, *Sliding distance of actin filament induced by a myosin crossbridge during one ATP hydrolysis cycle*, Nature, **316**, 366–369, 1985.

82. H.-L. YEH, T. HUANG, R. A. SCHACHAR, *A closed shell structured eyeball model with application to radial keratotomy*, J. Biomech. Engng., **122**, 505–510, 2000.

83. G. I. ZAHALAK, S. P. MA, *Muscle activation and contraction: constitutive relations based directly on cross-bridge kinetics*, J. Biomech. Engng., **112**, 52–62, 1990.

84. G. I. ZAHALAK, I. MOTABARZADEH, *A re-examination of calcium activation in the Huxley cross-bridge model*, J. Biomech. Engng., **119**, 20–29, 1997.

Received March 26, 2001.